Hindawi
International Journal of Antennas and Propagation
Volume 2023, Article ID 6825971, 11 pages
https://doi.org/10.1155/2023/6825971

Research Article

Application of the Finite Difference Parabolic Equation Model in Forestry Remote Telemetry

Qi Guo, Yubin Lan, Xiaoling Deng, and Yinliang Diao

Department of Electronic Engineering, South China Agricultural University, Guangzhou 510006, China

Correspondence should be addressed to Qi Guo; guoq36@mail2.sysu.edu.cn

Received 7 April 2023; Revised 30 June 2023; Accepted 5 July 2023; Published 1 August 2023

Academic Editor: Francesco D'Agostino

In this article, the finite difference parabolic equation (FDPE) method is presented to calculate the propagation loss (PL) for electromagnetic waves (EWs) in the forest environment. The FDPE method is more efficient and convenient than the empirical models and has more advantages on compatibility and accuracy for long-range EWs prediction. The Debye–Cole dual dispersion model is used to simulate the effective permittivity of vegetation. The results of the FDPE model are compared with those of the advanced refractive effects prediction system and measurement results, and a good agreement is observed. Research found that PL for EWs varies with the effective permittivity. Also, the effective permittivity is a function of radio frequency, weight moisture content, and volume content of vegetation. Thus, it is necessary to establish a statistical model to determine some relations between the PL and plant biophysical parameters. The polynomial fitting method is adopted to process a large amount of PL data for obtaining a linear function. Then, the volume content and moisture content of vegetation can be determined according to the polynomial fitting function. It provides a novel and efficient method for forestry remote telemetry, which is specifically suitable for large-scale inaccessible region with serious environment.

1. Introduction

With the development of communication network, remote telemetry technology is becoming more and more perfect. However, for the terrains that are complicated and inaccessible, traditional telemetry technology is unable to meet the needs of measurement, especially in the complex forest environment. The electromagnetic waves (EWs) can create different propagation properties near the surface of the different ground [1]. How to efficiently predict propagation loss (PL) distribution of EWs for a large-scale forest environment is the most important part [2].

Tamir first found that the forest can be equivalent to a lossy dielectric medium layer for radio propagation prediction [3]. When the transmitting and receiving antennas are situated within the vegetation, the direct EWs and ground-reflected EWs are dominant; the lateral EWs are tied to the forest-air interface. Also, a four-layer forest model can be used to predict the propagation loss at frequencies up to 2 GHz [4]. However, it is very hard to accurately calculate the PL in an actual forest because the PL values in the above models only depend on the frequency and propagation distance. In fact, the water content and volume rate of the plant have a significant influence on the PL distribution. Without taking vegetation's own biophysical factors into consideration, the above traditional models are not accurate for EWs propagation prediction in the forest environment.

In the current research, most propagation prediction models were just empirical models, which were applied in the wireless sensor network of precision agriculture. The commonly used empirical models are LITU-R, FITU-R, Cost 235, and log-normal [5]. It should be noted that these models were used in areas with foliage depths less than 1 km and were only explored the influence of the volume density of plants, ignoring the other factors, such as water content. Thus, the above empirical models used in the forest are limited. It is necessary to find an electromagnetic numerical model, which is more suitable for the large-scale complicated forest environment.

As is known to all, if we regard the forest as a loss dielectric layer, the PL values of EWs vary with the biophysical parameters of vegetation [6]. The effective permittivity is the main factor affecting PL, which is directly related to the volume content and moisture content parameters of plants. The Debye–Cole dual dispersion model was used to simulate the effective permittivity of forest [7]. The models regarded the forest as a mixture of air, water, and plants. It is found that the effective permittivity is a function of EWs frequency, moisture content, and volume content of plant. The more the moisture content and volume content, the higher the effective permittivity values of forest. With the increase in frequency, the effective permittivity is decreasing. The results show that the difference in effective permittivity will produce different EWs scattering, reflection, refraction, and diffraction effect. The research first reveals the linear relationship between the effective permittivity of plants and PL values of EWs.

However, it is essential to accurately predict the EWs distribution characteristics in the large-scale forest environment. The common electromagnetic numerical methods are geometrical optics (GO) and finite-difference time-domain (FDTD) [8, 9], which are suitable for simple scenarios and take longer computing time. They are inefficient and not appropriate for the forest environment. The PE method is an iterative electromagnetic numerical algorithm, which greatly reduces the calculation and improves the applicability in complicated environment. In recent years, the parabolic equation (PE) method has been widely used to model radio propagation in the troposphere [10–13].

In this paper, we present the finite difference parabolic equation (FDPE) method to predict the PL of EWs in the forest environment [14]. It has higher accuracy than the commonly used split-step Fourier transform (SSFT) parabolic equation method [15]. The FDPE is more convenient to solve the radio propagation problem in an in-homogeneous atmosphere.The results of FDPE model are compared with the advanced refractive effects prediction system (AREPS) [16] and measured data in literature [17], which verify its efficiency and superiority.

Based on the above results, the article will offer an innovative way for forest remote telemetry using large-scale EWs propagation. It is more convenient, efficient, and cost-effective than the traditional telemetry way. It involves just setting up the transmitter and receiver antennas in the woods. The polynomial fitting method is adopted to process a large number of PL sampled data obtained from the receiver. Then, the statistical model is established, and the volume content and moisture content parameters can be estimated according to the polynomial fitting function. The coefficient of determination R^2 is almost equal to 1. It proves that the fitting function has a great fit characteristic. The study provides a novel and efficient theoretical method for large-scale forestry remote telemetry.

2. Finite Difference Parabolic Equation Method for Radio Propagation

A brief description of the finite difference parabolic equation (FDPE) will be presented in this section [18].

In the two-dimensional Cartesian coordinates (x, z), we assume that the fields are independent of the y direction, where x and z correspond to the distance and height, respectively, and $\exp^{-i\omega t}$ is the time-dependence of the fields.

For horizontal polarization, the electric field E only has one nonzero component E_y, while for vertical polarization, the magnetic field H only has one nonzero component H_y. We work with the appropriate field component defined by

$$\psi(x,z) = E_y(x,z), \tag{1}$$

for horizontal polarization and

$$\psi(x,z) = H_y(x,z), \tag{2}$$

for vertical polarization. Also, the field component satisfies the following two-dimensional scalar wave equation:

$$\frac{\partial^2 \psi}{\partial x^2} + \frac{\partial^2 \psi}{\partial z^2} + k^2 n^2 \psi = 0, \tag{3}$$

where k is the free space wave number and n is the refractive index. We introduce the reduced functions associated with the paraxial direction x as follows:

$$u(x,z) = e^{-ikz}\psi(x,z). \tag{4}$$

Then, the scalar wave equation is given as follows:

$$\frac{\partial^2 u}{\partial x^2} + 2ik\frac{\partial u}{\partial x} + \frac{\partial^2 u}{\partial z^2} + k^2\left(m^2 - 1\right)u = 0, \tag{5}$$

where u represents a scalar component of the electric field for horizontal polarization or the magnetic field for vertical polarization, and m is the modified refractive index defined as follows:

$$m(x,z) = \left[n(x,z) - 1 + \frac{z}{a_e}\right] \times 10^6, \tag{6}$$

where a_e is the radius of the earth. The equation (5) can be formally written as follows:

$$\left[\frac{\partial u_+}{\partial x} + ik(1-Q)u_+\right]\left[\frac{\partial u_-}{\partial x} + ik(1+Q)u_-\right] = 0. \tag{7}$$

Here the wave equation is split into two terms, the u_+ and u_-, which represent, respectively, the forward and back propagating waves.

Then, the one-way PE is given as follows:

$$\frac{\partial u}{\partial x} + ik(1+Q)u = 0. \tag{8}$$

The pseudo-differential operator Q is given as follows:

$$\begin{aligned} Q &= \sqrt{\frac{1}{k^2}\frac{\partial^2}{\partial z^2} + m^2} = \sqrt{1+Z}, \\ Z &= \frac{1}{k^2}\frac{\partial^2}{\partial z^2} + m^2 - 1. \end{aligned} \tag{9}$$

The Q operator can be approximated by using the Greene form as follows:

$$Q = \sqrt{1+Z} \approx \frac{\chi_1 + \chi_2 Z}{\chi_3 + \chi_4 Z}. \tag{10}$$

Here, $\chi_1 = 0.99987$, $\chi_2 = 0.79624$, $\chi_3 = 1.00$, and $\chi_4 = 0.30102$. The Greene approximation FDPE can certainly give better results for irregular terrain [14].

Using the approximation in (10) for (8), the forward Greene approximation PE model can be written as follows:

$$\begin{aligned}
&\frac{\partial^3 u}{\partial x \partial z^2} + ik\left(1 - \frac{\chi_2}{\chi_4}\right)\frac{\partial^2 u}{\partial z^2} + k^2\left[\frac{\chi_3}{\chi_4} + \left(n^2 - 1\right)\right]\frac{\partial u}{\partial x} \\
&\quad = ik^3\left[\frac{\chi_1 - \chi_3}{\chi_4} + \left(\frac{\chi_2}{\chi_4} - 1\right)\left(n^2 - 1\right)\right]u.
\end{aligned} \tag{11}$$

In order to numerically solve (11), we need to transform the form of differential into difference. The resulting system to be solved by difference scheme is the pentadiagonal matrices as follows:

$$\begin{aligned}
&Tu_{j-2}^m - 16Tu_{j-1}^m + \left(D_j^m + d_j^m\right)u_j^m - 16Tu_{j+1}^m + Tu_{j+2}^m \\
&\quad = \tilde{T}u_{j-2}^{m-1} - 16\tilde{T}u_{j-1}^{m-1} + \left(D_j^m + \tilde{d}_j^m\right)u_j^{m-1} - 16\tilde{T}u_{j+1}^{m-1} + \tilde{T}u_{j+2}^{m-1},
\end{aligned} \tag{12}$$

where $j = 1, \ldots, Z$. Then, (12) is expressed by a matrix given as follows:

$$\begin{aligned}
&\begin{pmatrix}
\alpha_1^m & \phi_1^m & \varphi_1^m & & & & \\
\theta_2^m & \alpha_2^m & \phi_2^m & & & & \\
\vartheta_3^m & \theta_3^m & \alpha_3^m & & & & \\
\vdots & \vdots & \vdots & \ddots & \vdots & \vdots & \vdots \\
 & & & & \alpha_{Z-2}^m & \phi_{Z-2}^m & \varphi_{Z-2}^m \\
 & & & & \theta_{Z-1}^m & \alpha_{Z-1}^m & \phi_{Z-1}^m \\
 & & & & \vartheta_Z^m & \theta_Z^m & \alpha_Z^m
\end{pmatrix} \cdot
\begin{pmatrix} u_0^m \\ u_1^m \\ u_2^m \\ \vdots \\ u_{Z-2}^m \\ u_{Z-1}^m \\ u_Z^m \end{pmatrix} \\
&= \begin{pmatrix}
\tilde{\alpha}_1^m & \tilde{\phi}_1^m & \tilde{\varphi}_1^m & & & & \\
\tilde{\theta}_2^m & \tilde{\alpha}_2^m & \tilde{\phi}_2^m & & & & \\
\tilde{\vartheta}_3^m & \tilde{\theta}_3^m & \tilde{\alpha}_3^m & & & & \\
\vdots & \vdots & \vdots & \ddots & \vdots & \vdots & \vdots \\
 & & & & \tilde{\alpha}_{Z-2}^m & \tilde{\phi}_{Z-2}^m & \tilde{\varphi}_{Z-2}^m \\
 & & & & \tilde{\theta}_{Z-1}^m & \tilde{\alpha}_{Z-1}^m & \tilde{\phi}_{Z-1}^m \\
 & & & & \tilde{\vartheta}_Z^m & \tilde{\theta}_Z^m & \tilde{\alpha}_Z^m
\end{pmatrix} \cdot
\begin{pmatrix} u_0^{m-1} \\ u_1^{m-1} \\ u_2^{m-1} \\ \vdots \\ u_{Z-2}^{m-1} \\ u_{Z-1}^{m-1} \\ u_Z^{m-1} \end{pmatrix}.
\end{aligned} \tag{13}$$

The matrix elements ϑ_j^m, θ_j^m, α_j^m, φ_j^m, and ϕ_j^m in (13) can be written as follows:

$$\begin{aligned}
\vartheta_j^m &= T, \\
j &= 3 \cdots Z, \\
\theta_j^m &= \begin{cases} \left(\dfrac{48}{45 - 42\xi + 18\xi^2 - 4\xi^3} - 16\right)T \text{ for } j = 2, \\ -16T \text{ for } j = 3 \cdots Z. \end{cases} \\
\phi_j^m &= \begin{cases} \left(\dfrac{48 - 6\xi - \xi^3}{45 - 42\xi + 18\xi^2 - 4\xi^3} - 16\right)T \text{ for } j = 1, \\ -16T \; for \; j = 2 \cdots (Z - 1). \end{cases} \\
\alpha_j^m &= \begin{cases} \left(\dfrac{-723 + 54\xi + 18\xi^2 + 12\xi^3}{45 - 42\xi + 18\xi^2 - 4\xi^3}\right)T + \left(D_1^m + d_1^m\right) \text{ for } j = 1, \\ \left(\dfrac{-3}{45 - 42\xi + 18\xi^2 - 4\xi^3}\right)T + \left(D_1^m + d_1^m\right) \text{ for } j = 2, \\ \left(D_1^m + d_1^m\right) \text{ for } j = 3 \cdots Z. \end{cases} \\
\varphi_j^m &= T \; j = 1 \cdots (Z - 2).
\end{aligned} \tag{14}$$

Respectively, where the symbol T, D, and d are defined by the following equation:

$$\begin{cases}
T = 1 - ik\Delta x\left(\dfrac{\chi_2 - \chi_4}{2\chi_4}\right), \\
D_j^m = -\dfrac{12\Delta z^2 k^2}{\chi_4}\left[\chi_3 + \chi_4\left(\left(m_j^m\right)^2 - 1\right)\right], \\
d_j^m = 30T - \dfrac{6\Delta x \Delta z^2 ik^3}{\chi_4}\left[\left(\chi_3 - \chi_1\right) + \left(\chi_4 - \chi_2\right)\left(\left(m_j^m\right)^2 - 1\right)\right].
\end{cases} \tag{15}$$

We use the Leontovich boundary condition on the surface as follows:

$$\frac{\partial\left(\xi_m, 0\right)}{\partial z} = -ik\eta(x)u\left(\xi_m, 0\right). \tag{16}$$

The boundary field u $(x_m, 0)$ is found from

$$u_0^m = \frac{48u_1^m - 3u_2^m}{45 - 42\xi + 18\xi^2 - 4\xi^3}. \tag{17}$$

Then, the propagation loss (PL) of electric or magnetic fields u are defined by [18]

$$PL = -20\log_{10}|u| + 10\log_{10} d - 20\log_{10}\lambda + 20\log_{10}(4\pi), \tag{18}$$

where d is the horizontal propagation distance in km and λ is the wavelength in km. In the following experiments of Section 4, the PL values of EWs are calculated using equation (18).

3. Forest Propagation Environment Modeling

The calculation region of the forest propagation environment is divided into three layers: the absorbing layer, the air layer, and the loss dielectric layer, as shown in Figure 1.

The top absorbing layer is designed to eliminate the reflected waves coming from the upper boundary. Here, we will set the Tukey window function. The thickness of the absorbing layers is chosen to be 30% of the maximum height.

The air layer is in the middle of the calculation region, and the modified refractive index of the air layer is calculated using the equation (6).

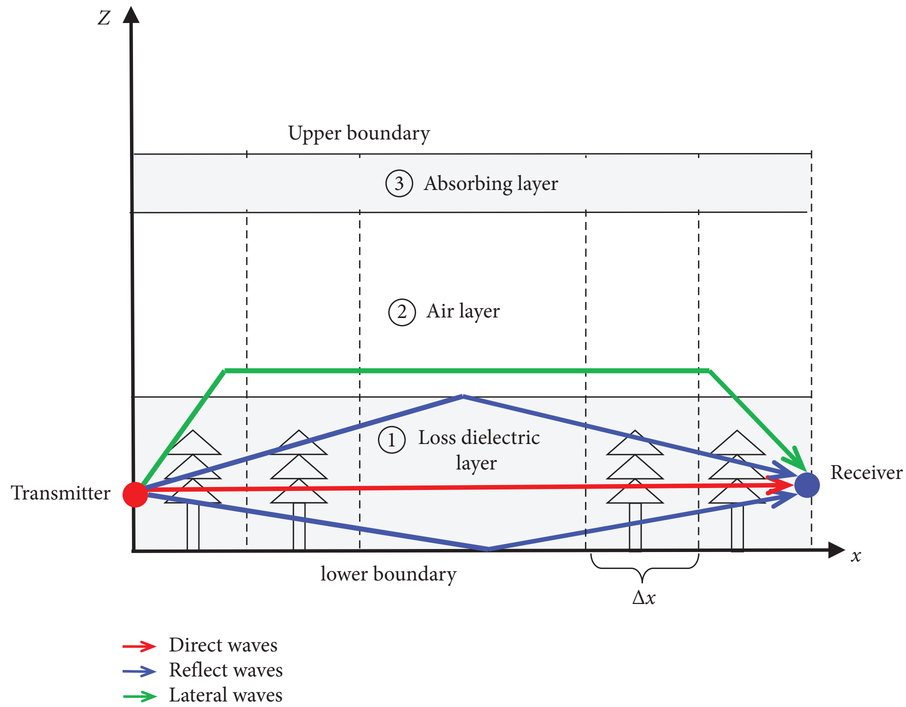

FIGURE 1: The hierarchy propagation model for the forest environment.

The lower layer is defined by the forest medium. When the EWs propagate in the forest environment, the vegetation can be considered as the lossy dielectric layer. The two-phase mixture refraction model regards the forest as a mixture of air and vegetation. The effective permittivity ε_e of forest is as follows [19]:

$$\varepsilon_e = \left[1 + V\left(\sqrt{\varepsilon_v} - 1\right)\right]^2, \tag{19}$$

where V represents the volume content of vegetation and ε_v the represents permittivity of vegetation.

According to the Debye–Cole dual dispersion model, the vegetation is considered as a mixture of plant, free water, and bound water. The permittivity of vegetation ε_v is defined by [7]

$$\varepsilon_v = \varepsilon_p + v_f \varepsilon_f + v_b \varepsilon_b. \tag{20}$$

Here, v_f and v_b represent the volume content of free water and bound water, respectively. v_f is defined as follows:

$$\begin{aligned} v_f &= M_v\left(0.82M_v + 0.166\right), \\ v_b &= \frac{31.4M_v^2}{\left(1 + 59.5M_v^2\right)}. \end{aligned} \tag{21}$$

The plant permittivity is ε_p, and the free water permittivity ε_f and the bound water permittivity ε_b are defined as follows:

$$\varepsilon_f = 4.9 + \frac{75}{(1 + \text{if}/18)} - i\left(\frac{18\sigma}{f}\right), \tag{22}$$

$$\varepsilon_b = 2.9 + 55\left(1 + \sqrt{\frac{\text{if}}{0.18}}\right), \tag{23}$$

where the unit of frequency f is GHz, and σ indicates the conductivity of the free water. It can be represented by the salinity S as follows:

$$\sigma = 0.16S - 0.0013S^2. \tag{24}$$

Here, salinity S is 8.5%. The volumetric moisture content M_v can be represented by weight moisture content M_g as follows:

$$M_v = M_g\left(0.55M_g - 0.076\right) + \frac{4.64M_g^2}{\left(3 + 22.08M_g^2\right)}. \tag{25}$$

In Figures 2 and 3, the relations between the effective permittivity and frequency f and volume content V and moisture content M_g are shown. The effective permittivity in Figures 2 and 3 is correlated with the equation (19). It shows that the effective permittivity is a function of the frequency, weight moisture content, and volume content of plant. The moisture contents are from 40% to 80%, the volume content is from 0.1% to 1%, and the frequency is 200 MHz and 300 MHz, respectively. It is found that the higher the moisture content and volume content, the higher is the effective permittivity and the effective permittivity increases with decreasing frequency.

4. Numerical Results and Discussion

In this section, the FDPE model is applied to a radio propagation simulation experiment in the forest environment. The results of FDPE model are compared with the advanced refractive effects prediction system (AREPS) [16] and measured data in literature [17], which verify its efficiency and superiority.

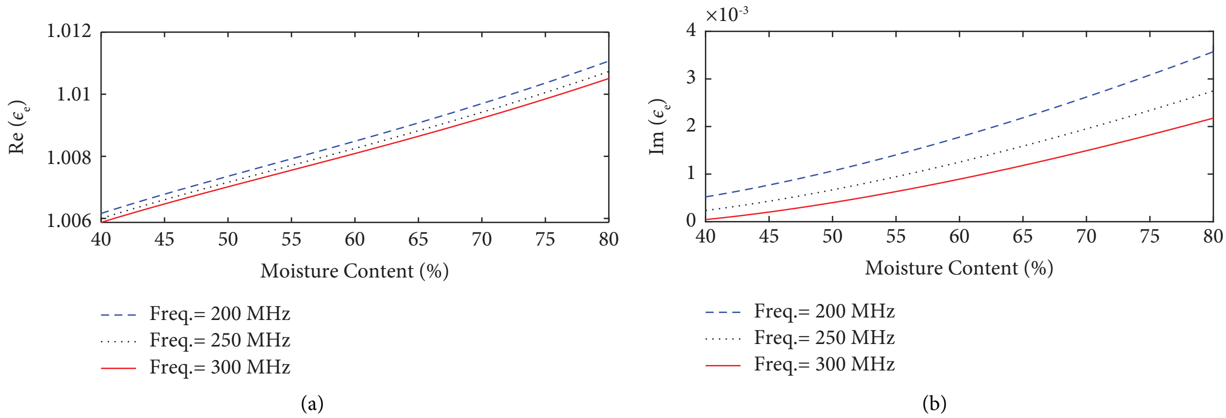

FIGURE 2: The relationship between the effective permittivity and moisture content. (a) Real part of effective permittivity. (b) Imaginary part of effective permittivity.

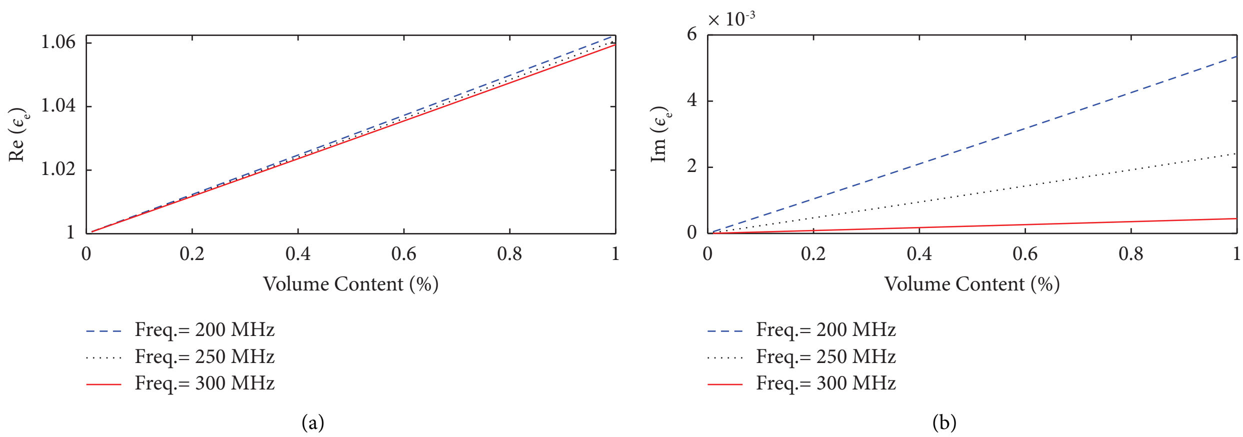

FIGURE 3: The relationship between the effective permittivity and volume content. (a) Real part of effective permittivity. (b) Imaginary part of effective permittivity.

The simulation conditions are set as follows: In the standard atmosphere, the transmitter is a Gaussian horizontally polarized (HP) antenna at a height of 10 m. The frequency is 300 MHz, and the half-power beam width is 3° with an inclination angle of 0°. The maximum distance is 10 km, and the maximum height is 3 km. The horizontal step Δx and vertical step Δz are normally set to be one-half of the wavelength. Suppose the type of ground is moderately dry. The relative permittivity is $\varepsilon_g = 20$, and the conductivity is $\sigma_g = 0.01$ S/m. The thickness of the forest dielectric layer is 15 m.

First, the FDPE model is compared with the AREPS to prove the validity in Figure 4. Suppose the surface types of bare ground and forest cover are both moderately dry ground. The volume content is set to 0.1%, the moisture content is set to 40%, and the effective permittivity is $1.0059 + 4.36e - 5i$. The results of the FDPE model are compared with those of AREPS, and a good agreement is observed. It is shown that forward EWs mainly propagate in the form of lateral waves in the forest environment, and the PL of lateral waves increases with the horizontal distance. Due to the effect of the lateral waves, the PL values in forest-covered environment are significantly reduced compared to the PL values in bare ground environment.

Then, the FDPE model is compared with measurements in Figures 5 and 6. The measured data used were carried out by Holm in a fir forest environment [17]. The frequency is 1355.5 MHz, and the forest is distributed near the ground and its thickness is about 18 m. The effective permittivity is $1.003 + 0.16e - 3i$ in the reference. Assuming the effective permittivity is set to be $1.003 + 0.16e - 3i$, $1.003 + 0.03e - 3i$, and $1.4 + 0.16e - 3i$, respectively, in our studies. The results show that PL values of EWs vary with the different effective permittivity. The difference in PL is very high below the height of 18 m. This is because the different characteristics of the forest will significantly affect the PL distribution. With increasing real and decreasing imaginary parts of effective permittivity, the PL decreased. However, the PL curves are found to be in excellent agreement beyond the height of 18 m. Because there is no forest and radio waves propagate in the air medium, the PL values are almost same over the top of the forest.

Second, the influence of moisture content of vegetation on the PL distribution is discussed in Figure 7. The thickness of

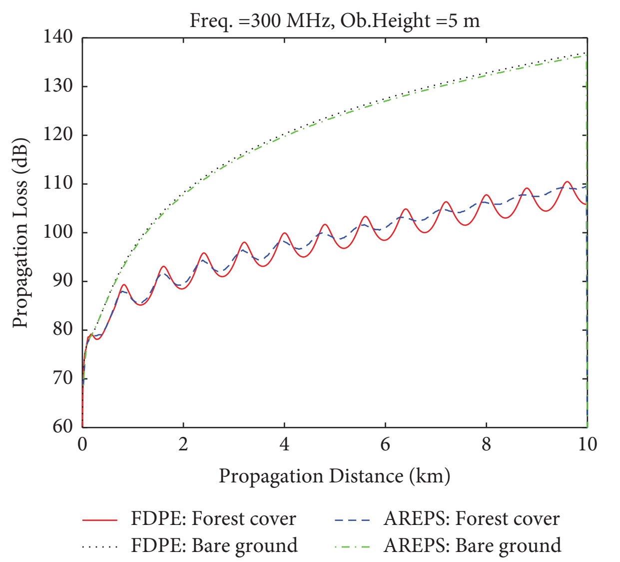

FIGURE 4: Comparison between the FDPE and AREPS in different environment.

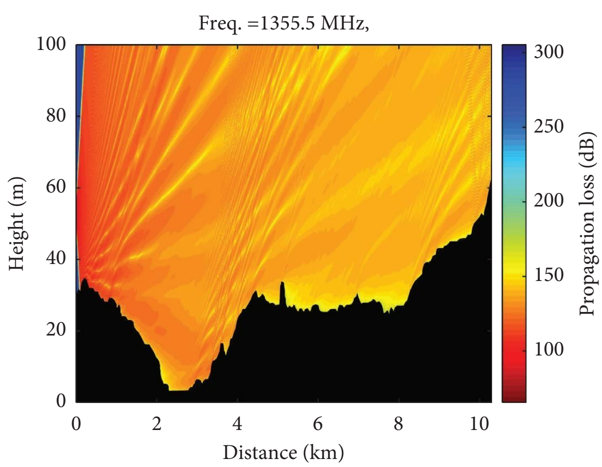

FIGURE 5: PL distribution using the FDPE model for the irregular forest environment.

the forest is 15 m, and the height of the transmitter antenna is 10 m. The volume content is set to be 0.1%. Assuming the moisture content is 40%, 43%, 47%, and 50%, then the effective permittivity is $1.0059 + 4.36e - 5i$, $1.0062 + 13.34e - 5i$, $1.0067 + 27.70e - 5i$, and $1.0070 + 40.04e - 5i$, respectively. The results show that EWs mainly propagate in the form of lateral waves in the forest. It is also found that when the moisture content of vegetation changed, the action range of lateral waves changed. Because the higher the moisture content, the faster the attenuation speed of lateral waves, and the smaller the action scope of lateral waves.

Third, the influence of volume content of vegetation on the PL distribution is discussed in Figure 8. Other simulation conditions are the same as above. The moisture content is set at 40%. Assuming the volume content is set to be 0.1%, 0.3%, 0.5%, and 0.7%, then the effective permittivity is

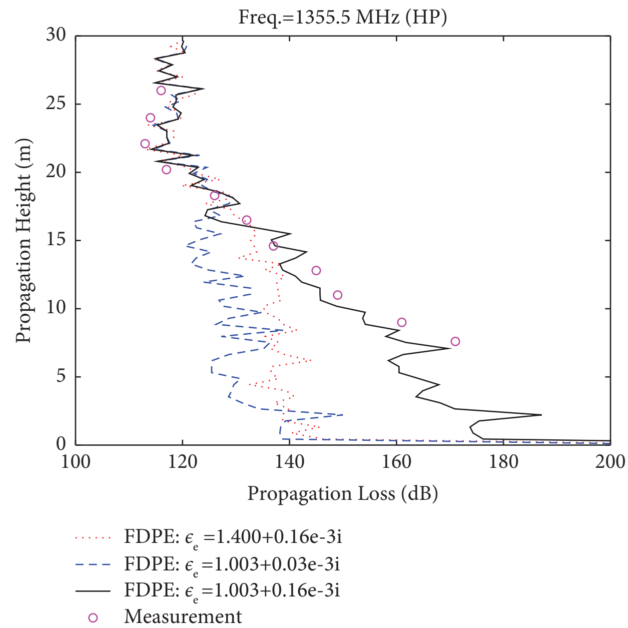

FIGURE 6: Comparison between the FDPE model and measurements.

$1.0059 + 4.36e - 5i$, $1.0177 + 13.18e - 5i$, $1.0295 + 22.09e - 5i$, and $1.0415 + 31.11e - 5i$, respectively. The real and imaginary parts of effective permittivity both increased with increasing volume content. It is shown that the higher the volume content, the larger the propagation loss.

In Figures 9 and 10, the PL curves along with distance are shown for different moisture content and volume content. The intense oscillation appears at the boundary of lateral waves' distribution areas. With increasing moisture content, the action scope of lateral waves decreased (Figure 9). It is found that as the volume content gets larger, the whole PL curves move upward to a higher level and oscillation becomes more intense in Figure 10. This is because there are larger real parts of effective permittivity for volume content values of 0.5% and 0.7%. The results show that the larger real parts of effective permittivity have greater impact on the superposition effect of reflection, refraction, and lateral waves.

In Figures 11 and 12, the PL curves along with height are shown for different moisture content and volume content. At the receiver location of 10 km, it is shown that the lower the moisture content and volume content, the smaller the PL values are. Furthermore, due to the fact that real part of effective permittivity varied in a larger range, the amplitude oscillation of PL curves became more intense with increasing volume content (Figure 12). It provides a theoretical basis for remote telemetry of moisture content and volume content values of vegetation for a large-scale forest environment.

In view of the above experiment results, it is shown that the vegetation's biophysical factors have a direct influence on the PL of EWs. It is necessary to establish a statistical model to determine some relations between PL values and moisture content or volume content.

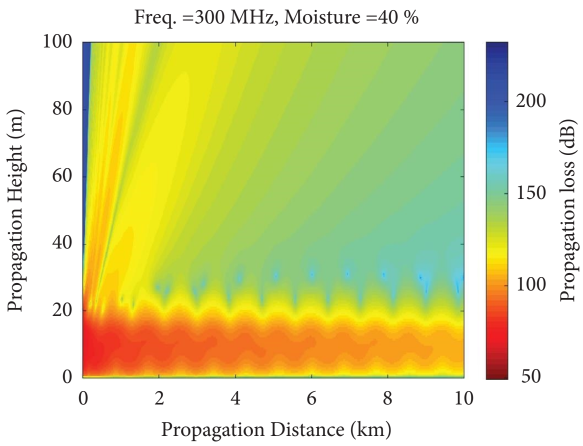

(a)

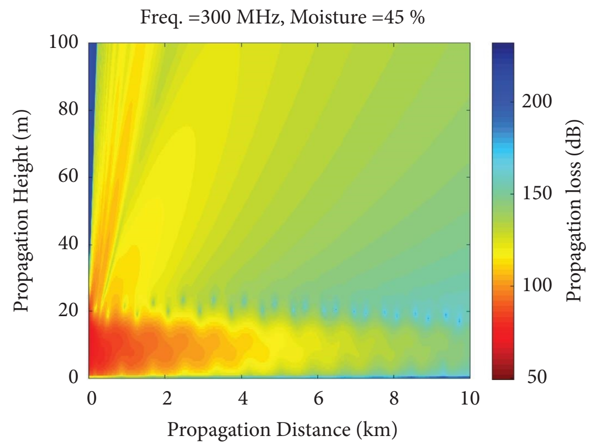

(b)

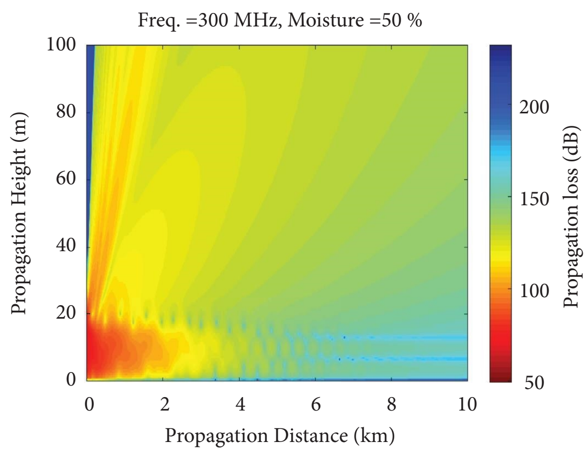

(c)

Figure 7: PL distribution for the different moisture content of vegetation. (a) Mg = 40% ($\varepsilon_e = 1.0059 + 4.36e - 5i$). (b) Mg = 45% ($\varepsilon_e = 1.0065 + 20.20e - 5i$). (c) Mg = 50% ($\varepsilon_e = 1.0070 + 40.04e - 5i$).

The polynomial fitting curve is the perfect linear evaluation method. It guarantees both the accuracy and reliability of the experimental results. Also, it is a simple and convenient empirical way which is given as follows:

$$f(x,\omega) = \sum_{j=0}^{N} \omega_j x^j \; N < m - 1. \quad (26)$$

Here, the polynomial fitting order $N = 3$, and m represents the number of sampling points. The other simulation conditions are unchanged. Suppose the receiving point is located at a distance of 10 km and a height of 10 m.

In Figure 13, the moisture contents are set to be 40%, 41%, 42%, and 43%, and the three-order polynomial fitting curves of PL along with the volume content are obtained, respectively. The corresponding fitting parameters are given in Table 1. The results show that the higher the moisture content, the higher the effective permittivity. Furthermore, it is found that the greater the volume content, the larger the PL values. In addition, it is shown that with increasing moisture content, the PL curves showed increasing trends. The absolute values of polynomial fitting coefficients ω_0, ω_1, and ω_3 decreased and ω_2 increased with increasing moisture content. The coefficient of determination (R^2) values tend to rise with increasing moisture content.

In Figure 14, the volume content ranges from 0.05% to 0.25% at intervals of 0.05%, and the corresponding PL curves along with the moisture content are shown, and the corresponding fitting parameters are given in Table 2. It is found that the higher the volume content, the higher is the effective permittivity. With increasing volume content, the PL curves showed increasing trends. The absolute value of polynomial fitting coefficients ω_0, ω_1, ω_2, and ω_3 increased with volume content increase. The coefficient of determination (R^2) values tend to descend with increasing volume content. The MAE and MAPE values tend to rise with increasing volume content. However, the coefficient of determination (R^2) values are almost equal to 1, which have great fitting characteristics.

According to the above two polynomial fitting curves, the volume content and moisture content parameters can be determined. The results show that the FDPE method is specifically suitable for propagation prediction in large-scale inaccessible regions with serious environment. It provides novel and efficient theoretical method for forestry remote telemetry.

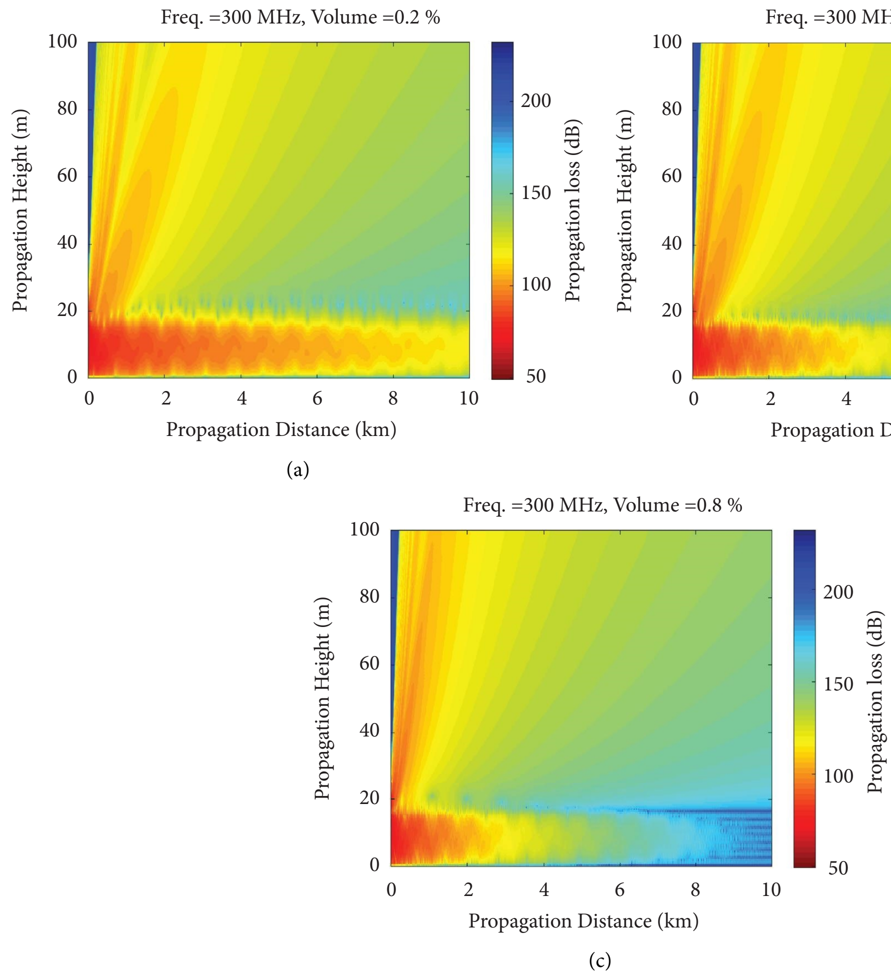

Figure 8: PL distribution for the different volume content of vegetation. (a) $V = 0.2\%$ $(\varepsilon_e = 1.0118 + 8.76e - 5i)$. (b) $V = 0.5\%(\varepsilon_e = 1.0295 + 22.09e - 5i)$. (c) $V = 0.8\%$ $(\varepsilon_e = 1.0475 + 35.65e - 5i)$.

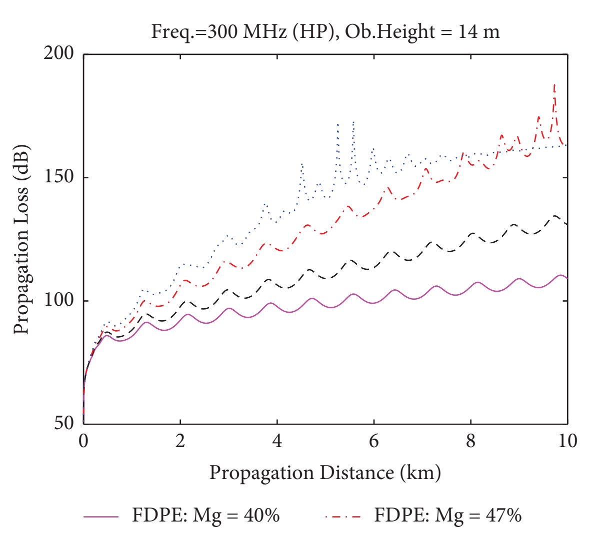

Figure 9: The relationship between PL and distance with different moisture content.

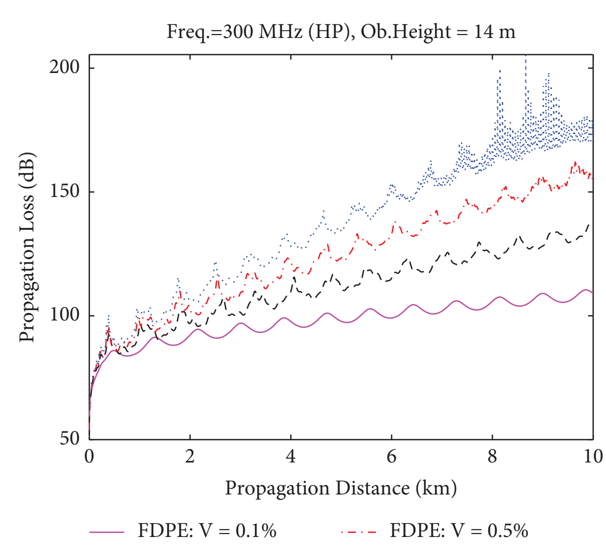

Figure 10: The relationship between PL and distance with different volume content.

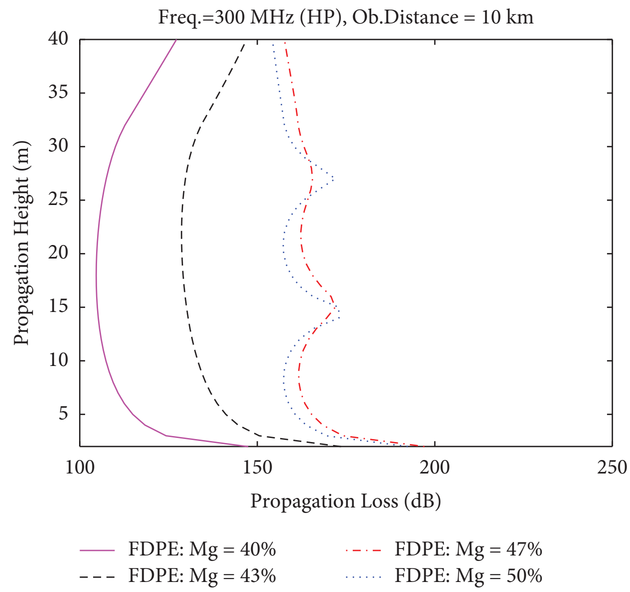

Figure 11: The relationship between PL and height with different moisture content.

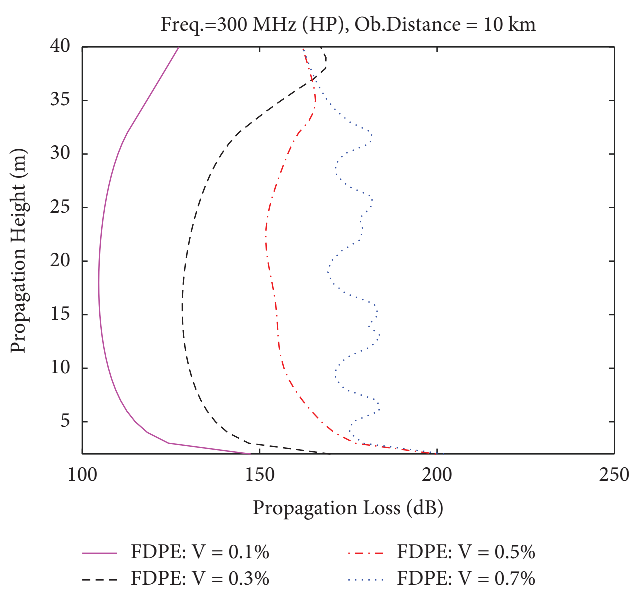

Figure 12: The relationship between PL and height with different volume content.

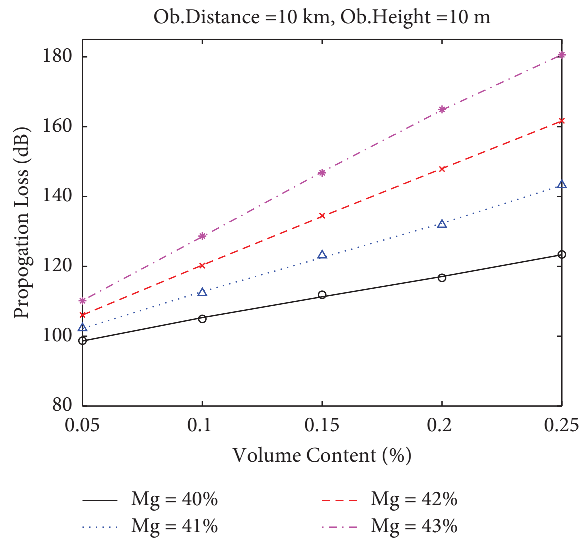

Figure 13: Polynomial fitting curves of PL with different moisture content.

Table 1: Fitting coefficients for the different moisture content.

Moisture content (%)	Effective permittivity $\varepsilon_{e(\mathrm{Min})}$	$\varepsilon_{e(\mathrm{Max})}$	Polynomial fitting coefficients ω_0	ω_1	ω_2	ω_3	MAE	MAPE (%)	R^2
40	$1.0029 + 2.18e - 5i$	$1.0147 + 10.96e - 5i$	−0.4613	3.1338	0.1139	95.9517	0.3069	0.2768	0.9983
41	$1.0030 + 3.58e - 5i$	$1.0150 + 18.01e - 5i$	−0.4607	3.1136	3.8798	95.7436	0.3389	0.2783	0.9992
42	$1.0031 + 5.07e - 5i$	$1.0153 + 25.53e - 5i$	−0.1814	1.1724	11.8743	93.2278	0.1117	0.0842	1.0000
43	$1.0031 + 6.66e - 5i$	$1.0156 + 33.51e - 5i$	0.0769	−0.6622	19.9601	90.7919	0.1401	0.0970	1.0000

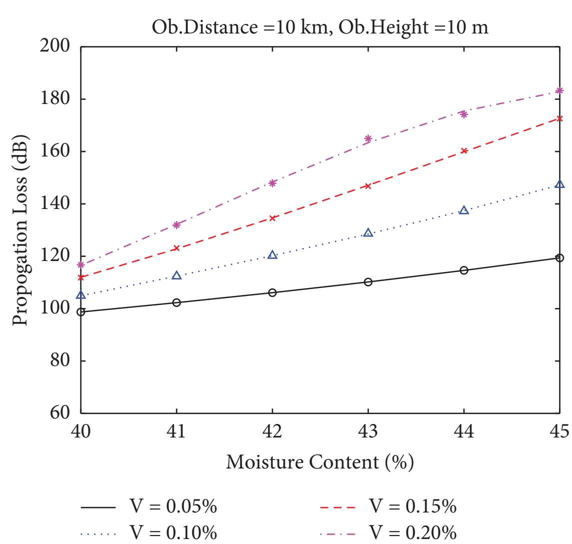

Figure 14: Polynomial fitting curves of PL with different volume content.

Table 2: Fitting coefficients for different volume content.

Volume content (%)	Effective permittivity $\varepsilon_{e(\mathrm{Min})}$	$\varepsilon_{e(\mathrm{Max})}$	Polynomial fitting coefficients ω_0	ω_1	ω_2	ω_3	MAE	MAPE (%)	R^2
0.05	$1.0029 + 2.18e - 5i$	$1.0032 + 10.08e - 5i$	0.0060	0.0881	3.2544	95.3743	0.0118	0.0107	1.0000
0.10	$1.0059 + 4.36e - 5i$	$1.0065 + 20.20e - 5i$	0.0328	−0.0595	7.4703	97.4674	0.0903	0.0704	0.9999
0.15	$1.0088 + 6.56e - 5i$	$1.0097 + 30.35e - 5i$	−0.0533	0.8019	8.8257	102.3991	0.2409	0.1704	0.9998
0.20	$1.0118 + 8.76e - 5i$	$1.0130 + 40.53e - 5i$	−0.2875	1.9938	11.6821	103.1542	0.7008	0.4337	0.9986

5. Conclusions

This article presents the finite difference parabolic equation method to calculate the propagation loss for electromagnetic waves in the forest environment. The results were compared with those of the AREPS and measurements, and good agreement was observed. It is found that propagation loss of EWs varies with the effective permittivity of vegetation, which is directly related to the biophysical parameters, including the volume content and moisture content. The polynomial fitting method is adopted to establish a statistical model to determine some relations between them. Then the volume content and moisture content of vegetation can be determined according to the polynomial fitting function. These studies provide a novel theoretical method for remote telemetry in a large-scale complicated forest environment.

Data Availability

No underlying data were collected or produced in this study.

Conflicts of Interest

The authors declare that there are no conflicts of interest.

Acknowledgments

This work was supported by the National Natural Science Foundation of China (Grant no. 61901532) and the National Defense Basic Research Program (JCKY2020210C614240301).

References

[1] Y. S. Meng, Y. H. Lee, and B. C. Ng, “Investigation of rainfall effect on forested radio wave propagation,” *IEEE Antennas and Wireless Propagation Letters*, vol. 7, pp. 159–162, 2008.
[2] G. Apaydin and L. Sevgi, “Fem-based surface wave multimixed-path propagator and path loss predictions,” *IEEE Antennas and Wireless Propagation Letters*, vol. 8, pp. 1010–1013, 2009.
[3] T. Tamir, “On radio-wave propagation in forest environments,” *IEEE Transactions on Antennas and Propagation*, vol. 15, no. 6, pp. 806–817, 1967.
[4] M. S Mikhailov, E. S Malevich, and V. A Permyakov, “Modeling of radio–wave propagation in forest by the method of parabolic equation,” *International Journal of Engineering & Technology*, vol. 7, no. 2.23, pp. 111–113, 2018.
[5] Y. S. Meng, Y. H. Lee, and B. C. Ng, “Empirical near ground path loss modeling in a forest at VHF and UHF bands,” *IEEE Transactions on Antennas and Propagation*, vol. 57, no. 5, pp. 1461–1468, 2009.
[6] G. L. Ramos and P. T. Pereira, “Analysis of radiowave propagation in forest media using the parabolic equation,” in *Proceedings of the 14th European Conference on Antennas and Propagation (EuCAP)*, Copenhagen, Denmark, March 2020.
[7] F. T. Ulaby and M. El-rayes, “Microwave dielectric spectrum of vegetation-Part II: dual-dispersion model,” *IEEE Transactions on Geoscience and Remote Sensing*, vol. 25, no. 5, pp. 550–557, 1987.
[8] D. A. McNamara, C. W. I. Pistorius, and J. A. G. Malherbe, *Introduction to the Uniform Geometrical Theory of Diffraction*, Artech House, Norwood, MA, USA, 1990.
[9] Z. El Ahdab and F. Akleman, “An efficient 3-D FDTD-PE hybrid model for radio wave propagation with near-source obstacles,” *IEEE Transactions on Antennas and Propagation*, vol. 67, no. 1, pp. 346–355, 2019.
[10] H. Oraizi and S. Hosseinzadeh, “Determination of the effect of vegetation on radiowave propagation by the Parabolic Equation Method,” *IEICE-Transactions on Info and Systems*, vol. 89, pp. 353–361, 2003.
[11] P. D. Holm and A. Waern, “Wave propagation over a forestedge- parabolic equation modelling vs. GTD modelling,” *IEEE International Symposium on Electromagnetic Compatibilities*, vol. 2, pp. 764–767, 2003.
[12] G. Apaydin and L. Sevgi, *Radio Wave Propagation and Parabolic Equation Modeling*, Wiley-IEEE Press, Hoboken, NJ, USA, 2017.
[13] A. A. Volkova and E. S. Malevich, “Modelling forest vegetation by single trees using parabolic equation method,” in *Proceedings of the International Youth Conference on Radio Electronics, Electrical and Power Engineering (REEPE)*, Moscow, Russia, March 2019.
[14] Q. Guo, C. Zhou, and Y. L. Long, “Greene approximation wide-angle parabolic equation for radio propagation,” *IEEE Transactions on Antennas and Propagation*, vol. 65, no. 11, pp. 6048–6056, 2017.
[15] G. Apaydin and L. Sevgi, “A Novel split-step parabolic-equation package for surface-wave propagation prediction along multiple mixed irregular-terrain paths,” *IEEE Antennas and Propagation Magazine*, vol. 52, no. 4, pp. 90–97, 2010.
[16] W. L. Patterson, “Advanced refractive effects prediction system (AREPS),” in *Proceedings of the IEEE Radar Conference*, pp. 891–895, New York, NY, USA, April 2007.
[17] P. D. Holm, G. Eriksson, and P. Kraus, “Wave propagation over a forest edge-parabolic equation modelling vs. measurements,” in *Proceedings of the 13th IEEE International Symposium on Personal, Indoor and Mobile Radio Communications*, pp. 140–145, Lisboa, Portugal, September 2002.
[18] M. Levy, *Parabolic Equation Methods for Electromagnetic Wave Propagation*, IEE, London, UK, 2000.
[19] M. L. Palud, “Propagation modeling of vhf radio channel in forest environment,” in *Proceedings of the IEEE MILCOM 2004. Military Communications Conference*, Monterey, CA, USA, November 2004.